

• Original Paper •

Characterization and Propagation of Historical and Projected Droughts in the Umatilla River Basin, Oregon, USA[✳]

Sudip GAUTAM¹, Alok SAMANTARAY², Meghna BABBAR-SEBENS¹, and Meenu RAMADAS²

¹*School of Civil and Construction Engineering, Oregon State University, Corvallis, OR 97331, USA*

²*School of Infrastructure, Indian Institute of Technology, Bhubaneswar, Odisha 752050, India*

(Received 18 October 2022; revised 22 February 2023; accepted 28 February 2023)

ABSTRACT

Climate change is expected to have long-term impacts on drought and wildfire risks in Oregon as summers continue to become warmer and drier. This paper investigates the projected changes in drought characteristics and drought propagation in the Umatilla River Basin in northeastern Oregon for mid-century (2030–2059) and late-century (2070–2099) climate scenarios. Drought characteristics for projected climates were determined using downscaled CMIP5 climate datasets from ten climate models and Soil and Water Assessment Tool to simulate effects on hydrologic processes. Short-term (three months) drought characteristics (frequency, duration, and severity) were analyzed using four drought indices, including the Standardized Precipitation Index (SPI-3), Standardized Precipitation-Evapotranspiration Index (SPEI-3), Standardized Streamflow Index (SSI-3), and the Standardized Soil Moisture Index (SSMI-3). Results indicate that short-term meteorological droughts are projected to become more prevalent, with up to a 20% increase in the frequency of SPI-3 drought events. Short-term hydrological droughts are projected to become more frequent (average increase of 11% in frequency of SSI-3 drought events), more severe, and longer in duration (average increase of 8% for short-term droughts). Similarly, short-term agricultural droughts are projected to become more frequent (average increase of 28% in frequency of SSMI-3 drought events) but slightly shorter in duration (average decrease of 4%) in the future. Historically, drought propagation time from meteorological to hydrological drought is shorter than from meteorological to agricultural drought in most sub-basins. For the projected climate scenarios, the decrease in drought propagation time will likely stress the timing and capacity of water supply in the basin for irrigation and other uses.

Key words: Umatilla, drought, SPI, SPEI, SSI, SSMI

Citation: Gautam, S., A. Samantaray, M. Babbar-Sebens, and M. Ramadas, 2024: Characterization and propagation of historical and projected droughts in the Umatilla River Basin, Oregon, USA. *Adv. Atmos. Sci.*, **41**(2), 247–262, <https://doi.org/10.1007/s00376-023-2302-8>.

Article Highlights:

- Droughts are projected to be more prevalent in the Umatilla River Basin under future projected conditions.
- Spatial variability in meteorological drought characteristics (SPI and SPEI) illustrate multiple levels of climatic stresses in the basin.
- Drought propagation from meteorological to hydrological drought is shorter than meteorological to agricultural drought by an average of two months.

1. Introduction

Drought is a creeping natural disaster that develops slowly and quietly over time (van Loon, 2015; Mukherjee et al., 2018; Ault, 2020). Drought affects a large portion of the population and is one of the most damaging natural disasters

(Zhao and Dai, 2015). Drought is typically defined as a period of time with prolonged dryness resulting mostly from lower than “normal” precipitation (Mishra and Singh, 2010; Ding et al., 2011). “Normal” precipitation refers to the average precipitation value over a span of 30 years. Drought is an expensive disaster, costing the United States approximately \$285.4 billion between 1980 and 2021 (NOAA National Centers for Environmental Information, 2022).

Precipitation and temperature are the main drivers of drought as they largely determine the levels of snowpack, soil moisture, and streamflow. These drivers are commonly

✳ This paper is a contribution to the special issue on Causes, Impacts, and Predictability of Droughts for the Past, Present, and Future.

* Corresponding author: Sudip GAUTAM
Email: gautams@oregonstate.edu

used in drought indicators (Oregon.gov, 2021). Physical droughts can be divided into three categories: meteorological drought, hydrological drought, and agricultural drought. Meteorological droughts are typically associated with precipitation deficits (Li et al., 2017), and are defined based on the degree of dryness compared to the “normal” amount and the duration of the dry period (National Drought Mitigation Center, 2021). Hydrological drought results from the effects of precipitation deficit on the surface or subsurface water supply and affect streamflow, lakes, ponds, etc. (Li et al., 2017; National Drought Mitigation Center, 2021). Agricultural drought results from soil moisture deficit. The deficits from meteorological drought can propagate through hydrological processes and interactions at the catchment scale to yield deficits for hydrological and agricultural droughts (Apurv et al., 2017; Zhang et al., 2022).

Drought indicators are parameters used to describe drought conditions (Drought.gov, 2021), e.g., precipitation, temperature, streamflow, soil moisture, snowpack, etc., whereas drought indices are the computed numerical representations of drought stress assessed using drought indicators (WMO and GWD, 2016) that help to gather meaningful insights on drought patterns from the respective time series data (National Drought Mitigation Center, 2022). The choice of a drought index for a particular study depends on the drought type and the required dataset's availability. Researchers have developed various indices to understand and characterize different types of droughts (WMO and GWD, 2016). Keyantash and Dracup (2002) evaluated the commonly used drought indices for the three types of physical drought for two regions in Oregon (Willamette Valley and North Central climate division) and identified rainfall deciles, total water deficit, and computed soil moisture as “superior” drought indices for meteorological, hydrological, and agricultural drought, respectively. In contrast, the U.S. Drought Monitor (USDM) uses a composite index that combines drought indicators across the hydrological cycle with information from local experts (Svoboda et al., 2002; Leeper et al., 2022). The USDM uses the Palmer Drought Severity Index (Palmer, 1965), Standardized Precipitation Index (SPI; McKee et al., 1993), various indicators for soil moisture and hydrology (USGS weekly streamflow), and satellite images to obtain an Objective Drought Indicator Blend and provide drought outlooks for the entire United States (Svoboda et al., 2002). It provides information on the drought intensity, affected area/population, and possible impacts in map and tabular form. However, it is not a drought forecast tool and only provides a monthly and seasonal drought outlook for up to three months.

In the western United States, droughts have chronically created deficits in the water supply over the last 22 years. Many states are currently experiencing a mega-drought amid an extremely dry year, heat waves, and record-breaking high temperatures (Williams et al., 2022). For the Pacific Northwest state of Oregon, the fifth Oregon Climate Assessment Report (Dalton and Fleishman, 2021) projects that under the continuation of current levels of greenhouse gas

emission, the frequency of droughts is likely to increase as summers continue to become warmer and drier. Dalton and Fleishman (2021) also reported that for the period 2000–2020, about 37% of Oregon experienced moderate drought, whereas 7% of Oregon experienced extreme drought. For the severe drought in 2015, the state administration declared emergency drought declarations in 25 of its 36 counties (State of Oregon, 2016). Since then, the drought emergency declarations for the following years have been 2018–11 counties, 2020–15 counties, 2021–26 counties, and 2022–17 counties (Oregon Water Resources Department, 2022). Clifton et al. (2018) studied the effects of climate change on the hydrology and water resources in the Blue Mountains region of Oregon and reported that by the 2080s (2070–2099), diminished snowpack and low summer flows are likely to reduce water supply for aquatic ecosystems, agriculture, municipal consumption, and livestock grazing in areas lacking substantial groundwater.

Studies in the northwestern United States have also involved model-based analyses of drought projections that consider the effect of climate change. For example, Abatzoglou and Rupp (2017) evaluated 24 Coupled Model Intercomparison Project 5 (CMIP5) Global Climate Models (GCMs) in simulating regional droughts to help users with model selection. They found that CMIP5 models simulate regional drought in the northwestern United States reasonably well across different timescales. Ahmadalipour et al. (2017b) analyzed the performance of 20 CMIP5 GCMs in the Columbia River Basin (CRB) for climate change impact analysis using various univariate and multivariate methods. They ranked the performance of the climate models for different temporal scales (daily, monthly, and seasonal) and recommended the ten-best representative GCMs for the CRB. These GCMs Ahmadalipour et al. (2017b) were later used by Ahmadalipour et al. (2017a) to study the projected changes in meteorological and hydrological drought characteristics in the Willamette River Basin that lies within the larger Columbia River Basin.

This present study focuses on droughts in a complex socio-ecological system in the Umatilla River Basin (URB) in northeastern Oregon. The basin has been profoundly transformed from its natural state due to anthropogenic activities such as agriculture, water rights, and reservoir operations. This study considers the current situation of the URB to be a baseline scenario and analyzes how future scenarios compare to the present. The Umatilla River Basin has suffered droughts in the past, with Umatilla County submitting emergency declarations due to low water conditions and drought in 1992, 1994, 2002, 2003, 2005, 2015, and most recently, in 2021. Morrow County had emergency drought declarations in 1992, 2001–2005, 2013, 2015, 2018, 2020, 2021, and 2022. The main impacts of drought have been on agriculture, fish and wildlife, and increased fire risk. Although the region has been impacted by drought in the past and present, only a few studies have been conducted to understand the drought characteristics of the basin (Clifton et al., 2018; Dalton, 2020; Dalton and Fleishman, 2021). In particular, Dalton

(2020) studied the future climate projections in Umatilla County and summarized how it impacts precipitation, temperature, water availability, drought, and wildfire conditions in the county. This study aims to provide a detailed drought analysis by exploring various drought characteristics and drought propagation in the URB.

Specific objectives addressed by this study are as follows:

i) Evaluate and characterize the meteorological, hydrological drought, and agricultural drought indices in the Umatilla River Basin for historical (1981–2005) and projected future scenarios (2030–2059 and 2070–2099).

ii) Analyze and compare the drought propagation from meteorological to hydrological and agricultural droughts in the basin for the historical and projected climate scenarios.

2. Methodology

2.1. Study area

The Umatilla River Basin lies in northeastern Oregon and occupies a 2518 square mile area in the Middle Columbia Basin (Fig. 1). The URB is an agriculture-dependent basin with a semiarid climate characterized by low annual precipitation, low winter temperatures, and high summer temperatures. The basin is in Umatilla and Morrow counties, with most of the basin occupying Umatilla County. The

Umatilla River originates in the Blue Mountains region and flows west to the Columbia River, providing water for irrigation, water supply, agricultural use, industrial usage, etc., to the basin's residents along the way. Approximately 87 700 people live within the Umatilla Basin (Tilt et al., 2022), which includes the major population centers of Umatilla, Hermiston, Pendleton, Pilot Rock, and the Confederated Tribes of the Umatilla Indian Reservation (CTUIR). The mean annual precipitation varies from 205 mm to 1424 mm, with the eastern region of the basin receiving more precipitation than the west. The URB has more than 1000 farms and ranches, with approximately 20% of the farms bigger than 1000 acres (USDA, 2005). Around 23% of the land in the basin (378,600 acres) is used for cultivating grain crops, and 111 000 acres of the land is irrigated, including 64 200 acres of cultivated cropland (USDA, 2005). Irrigation water includes water from the Columbia River, Umatilla River, groundwater, and water stored upstream of the reservoirs. The region also consists of critical groundwater areas that have experienced extreme declines in the groundwater levels in both the alluvial and deep basalt aquifers (Oregon.gov, 2022).

For this study, the URB has been divided into four zones based on the location, stream network, water availability, land use, and drought characteristics of the sub-basins (Figs. 1a–d). Zone 1 is characterized by the presence of the Umatilla Indian Reservation, the Umatilla National Forest,

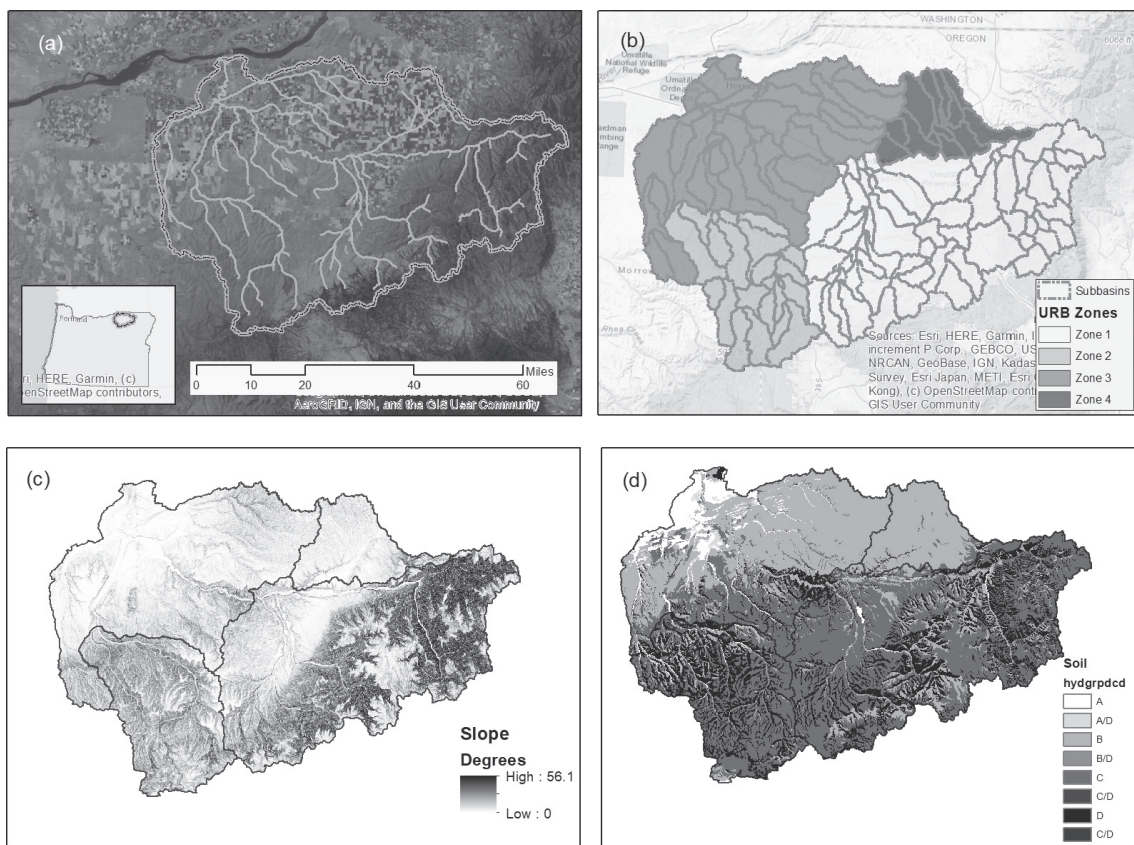


Fig. 1. Umatilla River Basin (a) location, land use, and stream network, (b) sub-basins and zones in the URB, (c) slope map, and (d) soil hydrologic group.

and the Blue Mountains. The major population center in Zone 1 is the city of Pendleton. Zone 2 is an underdeveloped zone that has mountainous terrain and is a data-scarce region. Little Butter creek lies in Zone 2, which is an important source of surface water in the region. Almost half of the area of Zone 2 lies in Morrow County. Zone 3 consists of major populated areas such as Hermiston, Umatilla, Stanfield, and Echo. This zone has major economic activities of the basin, including most of the agricultural production and food processing as well as the presence of industries and Amazon data centers. The Lower Umatilla Basin Groundwater Management Area (LUBGWMA) is also a part of Zone 3. Zone 4 primarily consists of an agricultural area, and Wildhorse Creek is a major source of surface water.

2.2. Climate data

In this study, we used the climate data from the Parameter-elevation Regressions on Independent Slopes Model (PRISM) and projected the climate data of the Umatilla River Basin from 10 different climate models (Table S1 in the Electronic Supplementary Materials, ESM). PRISM precipitation and temperature data from 1981–2019 were obtained from the PRISM group's website (<https://prism.oregonstate.edu/>). Daily gridded PRISM precipitation and temperature data (1981–2005) with a spatial resolution of 800 m is used for creating the baseline scenario. The climate projection data were obtained from Northwest Climate Toolbox (<https://climatetoolbox.org/>) for the same PRISM grid locations. Data obtained from the climate toolbox included Past Weather Data (1950–2005) and Future Climate Projection Data (2006–2099) for the CMIP5 Representative Concentration Pathways (RCPs) 4.5 and 8.5 scenarios of 10 GCMs. The 10 models used to obtain the projected future precipitation and temperature data include BCC-CSM1-1, CanESM2, CCSM4, GFDL-ESM2G, GFDL-ESM2M, Inmcm4, IPSL-CM5A-LR, IPSL-CM5A-MR, IPSL-CM5B-LR, and MIROC5, that were used in studies by Ahmadalipour et al. (2017b) and Ahmadalipour et al. (2017a). RCP 4.5 scenario represents intermediate stabilization pathways in which radiative forcing is stabilized at approximately 4.5 W m^{-2} after 2100, whereas the RCP 8.5 scenario represents a high-emission scenario in which radiative forcing reaches greater than 8.5 W m^{-2} after 2100 and continues to rise. All 10 GCMs were downscaled to $0.06^\circ \times 0.06^\circ$ spatial resolution using the Bias Correction and Spatial Disaggregation method (Wood et al., 2004).

2.3. SWAT model

A hydrologic model was developed for the URB using the Soil & Water Assessment Tool (SWAT) 2012 (Neitsch et al., 2011; Arnold et al., 2012, 2013). The SWAT model of the URB was calibrated for the historical timeframe (1981–2005) using the PRISM climate data for the basin. Calibrated SWAT parameters include snow parameters, groundwater parameters, management parameters, hydrologic response unit (HRU) parameters, soil parameters, routing parameters, and reservoir parameters (Table S2 in ESM).

The SWAT model of the URB consists of 147 sub-basins, and the streamflow was calibrated at 12 gaging stations and two reservoirs (Fig. S2 in the ESM). Once the model was calibrated for streamflows, reservoir storage, and crop yield, the SWAT model was run for historical and future climate scenarios using the Past Weather Data (1981–2005) for 10 models and corresponding future climate projections (2030–2059 and 2070–2099). To understand the impacts of climate change in the basin, certain assumptions regarding water extraction and crop rotation in the basin were made during the SWAT model simulations. For the SWAT model simulations in projected future conditions, it is assumed that the reservoir operations decisions from the calibrated model (historical period) are respected. Actual crop rotation in the basin from 2007–2018 was used to create the crop rotation cycle in the SWAT model, and this 12-year crop rotation cycle is assumed to stay constant between both historical and future simulations of the SWAT model. Additionally, it is assumed that water extraction from the Umatilla River tributaries into the irrigation ditches in the future scenarios (2030–2059 and 2070–2099) will remain the same as in the historical period (1981–2005). Monthly streamflow, potential evapotranspiration, and soil moisture output were extracted from the SWAT model simulations for further analysis.

2.4. Drought indices

Based on the literature review of previous studies, we selected the following indices to represent the various drought categories: Standardized Precipitation Index (SPI), Standardized Precipitation Evapotranspiration Index (SPEI) for meteorological drought, Standardized Streamflow Index (SSI) for hydrological drought, and Standardized Soil-moisture Index (SSMI) for agricultural drought.

The SPI is a universally used index for meteorological drought analysis due to its advantages such as simplicity (only uses precipitation), versatility (can be computed at various timescales for monitoring different droughts), and consistency (due to its normal distribution) (Hayes et al., 1999). However, the SPEI improves upon the SPI by considering evapotranspiration, and the authors of the SPEI argue that it is more reliable for climate change studies (Vicente-Serrano et al., 2010). Due to the lack of information on the effectiveness of these drought indices in the URB, it is important to study both the SPI and SPEI to understand and compare the drought characteristics to better inform stakeholders. Thus, we have considered these two indices for meteorological drought analysis. Computation of the drought indices was done using the standard methodology in practice. The USDM was not used as it has limited applicability in future scenarios and requires various data that are not easily accessible.

2.4.1. Standardized Precipitation Index (SPI)

McKee et al. (1993) developed the method used for SPI calculation to study the relative departures of precipitation from their “normal” amount. The procedure in SPI calculation involves the following steps: (i) precipitation data is fitted

to a gamma distribution; (ii) cumulative probability gamma function is transformed to a standard normal distribution; (iii) The SPI value is represented by the “z-score” in the standard normal distribution.

Monthly precipitation aggregates at various timescales (1, 3, 6, 12, 18, 24 months, etc.) can be used as input in calculating SPI values at the corresponding timescales. Drought occurs when the SPI value is continuously negative. Drought classification, based on SPI values as per McKee et al. (1993), includes four categories: mild drought (0 to -0.99), moderate drought (-1.00 to -1.49), severe drought (-1.50 to -1.99), and extreme drought (≤ -2.00).

The SPI at various accumulation periods can be used as an indicator for various impacts. For example, the SPI computed for shorter accumulation periods of 1 to 3 months can be used to indicate immediate impacts such as reduced soil moisture, snowpack, and flow in smaller creeks (European Commission, 2020). SPI values were computed for each sub-basin within the Umatilla River Basin based on the monthly precipitation values for the timescale of three months to analyze the short-term drought characteristics. The 3-month SPI compares the precipitation over a specific 3-month period with the precipitation totals for the same 3-month period of all the years. i.e., the 3-month SPI at the end of February compares the December-January-February precipitation total for a particular year with the December-February precipitation totals of all the years (Indiana Department of Natural Resources, 2022). As such, it reflects short-term trends in precipitation and moisture conditions.

In addition, SPI values were computed for the timescales of 1 through 20 months for the correlation analysis between drought indices.

2.4.2. Standardized Precipitation Evapotranspiration Index (SPEI)

The SPEI, as proposed by Vicente-Serrano et al. (2010), is computed using both the precipitation and temperature time series and involves the climatic water balance. The precipitation and temperature time series for different scenarios were used as input to the SWAT model, and the potential evapotranspiration (PET) was extracted from the SWAT

runs. Then, the deficit (D) of precipitation (P) and potential evapotranspiration was computed using Eq. (1)

$$D_i = P_i - PET_i \tag{1}$$

The monthly time series of deficit (D) for a month (i) is used to calculate the SPEI values using the same procedure as for the SPI. The normalized SPEI also has the same drought category classification as the SPI. SPEI values were also computed for each sub-basin for the 3-month timescale. Similar to the SPI, SPEI values were also computed for the timescales of 1 through 20 months for the correlation analysis.

2.4.3. Standardized Streamflow Index (SSI) and Standardized Soil-moisture Index (SSMI)

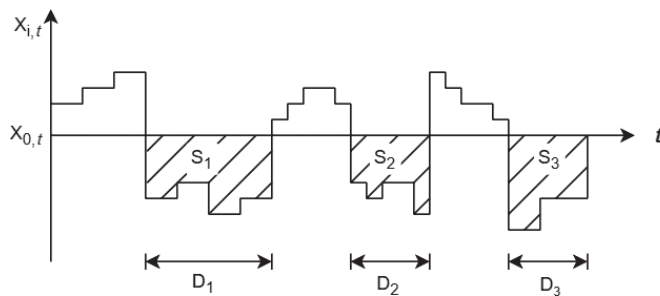
The Standardized Streamflow Index (SSI) (Modarres, 2007) and Standardized Soil-Moisture Index (SSMI) (Xu et al., 2018) are computed similarly to the SPI using the runoff and soil moisture time series in place of precipitation time series. They are calculated using the same gamma distribution and follow the same SPI drought category classification. Both the SSI and SSMI were also calculated for the 3-month timescale, similar to the SPI and SPEI, to study short-term drought characteristics.

2.5. Drought characteristics

Drought occurs when the value of drought indices (SPI, SPEI, SSI, SSMI) is negative. Drought characteristics are defined using run theory (Yevjevich, 1967) A drought event is defined as consecutive instances of drought, i.e., a set of consecutive months that have a negative value of the drought index (Fig. 2). Drought duration is calculated as the number of consecutive months that have a negative value for the drought index. Drought severity is calculated as the sum of the absolute values of the drought index for consecutive drought instances during an event (Kwak et al., 2016).

Droughts in the URB are characterized with the help of the following five parameters:

- i) Drought frequency: Total number of drought occurrences within the study period normalized by the number of years in the study



$X_{i,t}$: drought index at time t
 D_i : drought duration
 S_i : drought severity

Based on the figure and run theory, drought characteristics can be computed as given below:

- Drought Frequency = 3 (No. of drought occurrences)
- Average Drought Duration = $(D_1 + D_2 + D_3) / 3$
- Average Drought Severity = $(S_1 + S_2 + S_3) / 3$
- Maximum Drought Duration = $\text{Max}(D_1, D_2, D_3) = D_1$
- Maximum Drought Severity = $\text{Max}(S_1, S_2, S_3) = S_1$

Fig. 2. Drought severity, duration, and frequency (modified from Kwak et al., 2016).

- ii) Average Drought Duration: Average value of all the drought durations (D1, D2, D3) in months
- iii) Average Drought Severity: Average value of all the drought severities (S1, S2, S3)
- iv) Maximum Drought Duration: Maximum value of the drought durations (D1, D2, D3) in months
- v) Maximum Drought Severity: Maximum value of the drought severities (S1, S2, S3)

These drought characteristics have been computed for both the baseline and future periods under the RCP 4.5 and RCP 8.5 scenarios for all the drought indices. Drought characteristics have been computed for three time periods: Historical (1981–2005), Mid-Century (2030–2059), and Late-Century (2070–2099). To understand the effects of short-term (seasonal) anomalies of precipitation, evapotranspiration, streamflow and soil moisture on drought, drought characteristics are computed using drought indices with a timescale of three months, i.e., SPI-3, SPEI-3, SSI-3, and SSMI-3. An advantage of using the 3-month indices over a 1-month index is that it can reveal long-term deficits even during a wet month and inform whether a longer-term drought is still underway. Furthermore, studies have also found that meteorological drought indices with a 3-month timescale correlate well with agricultural drought (Sun et al., 2017, 2022).

2.6. Drought propagation

Drought propagation is defined as the change of the drought signal as it moves from anomalous meteorological conditions (precipitation deficit, increased evapotranspiration) to hydrological and agricultural droughts through the terrestrial parts of the hydrological cycle such as soil system, surface water, and groundwater bodies (van Loon, 2013; van Loon et al., 2015; Zhang et al., 2022). To characterize the propagation of drought from meteorological to hydrological and agricultural droughts in the URB, correlation analysis between the drought indicators has been used during the historical and projected climate scenarios. The purpose of the correlation analysis is to identify the drought propagation time. This response time represents the time for accumulated deficit in meteorological drought to correspond to the hydrological and agricultural droughts (Zhang et al., 2022). The Standardized Precipitation Index (SPI) and Standardized Runoff Index (SRI) are frequently used indices for understanding the propagation of meteorological drought to hydrological drought (Xu et al., 2019; Jehanzaib et al., 2020).

The drought propagation time (T_p) is identified using the maximum correlation between the drought indices (the

SPI and SSI for hydrological drought, SPI and SSMI for agricultural drought). The drought propagation time is based on the SPI scale (1–20 months). In this analysis, the Pearson correlation between the 3-month SSI and 3-month SSMI is computed with SPI of various scales (1–20 months). Then, the SPI scale at which the maximum correlation occurs is identified and represents the drought propagation time, as shown in Eqs. (2–4):

$$T_p = \operatorname{argmax}_n(f_n) , \tag{2}$$

$$\text{For SSI, } f_n = \operatorname{corr}(\text{SPI}_n, \text{SSI}_3); 1 \leq n \leq 20 , \tag{3}$$

$$\text{For SSMI, } f_n = \operatorname{corr}(\text{SPI}_n, \text{SSMI}_3); 1 \leq n \leq 20 . \tag{4}$$

3. Results and discussion

3.1. Long-term characteristics and trends in climate data

Long-term average monthly precipitation and temperature were estimated from the PRISM and downscaled GCM models data using the daily precipitation and temperature. Average annual precipitation and temperature calculated across the basin for different time periods are given in Table 1. Results from the analysis show a decline in the average projected precipitation over the basin and an increase in minimum and maximum temperatures during both the mid-century (2030–2059) and late-century (2070–2099) under both RCP 4.5 and RCP 8.5 conditions (Fig. S1 in the ESM).

Trend analysis of the climate data was done for all time periods (historical, mid-century, and late-century; RCP 4.5 and 8.5 scenarios) separately with the help of the Mann-Kendall trend test (Hussain and Mahmud, 2019) using a 5% significance level. Statistically significant increasing temperature trends (both minimum and maximum) and no significant trend in precipitation were observed in the basin during all the scenarios (Table S3 in the ESM). Similarly, trend analysis was carried out at the zonal level. No trend in precipitation was found in any zone for all the scenarios. In contrast, the temperature (both minimum and maximum) showed an increasing trend in the basin for all the scenarios. The long-term observations and trends in this study agree with the previous climate change studies for this region, where an increasing temperature trend and no significant precipitation trend

Table 1. Long-term precipitation (pcp), minimum (tmin) and maximum (tmax) temperature values in the URB.

Time	Scenario	pcp (mm)	tmin (°C)	tmax (°C)
Historical (1981–2005)	PRISM	936	0.64	10.99
	Models	900	–1.52	12.08
Mid-century (2030–2059)	RCP 4.5	817	1.47	12.80
	RCP 8.5	809	1.90	13.23
Late-century (2070–2099)	RCP 4.5	819	2.15	13.57
	RCP 8.5	851	4.22	15.71

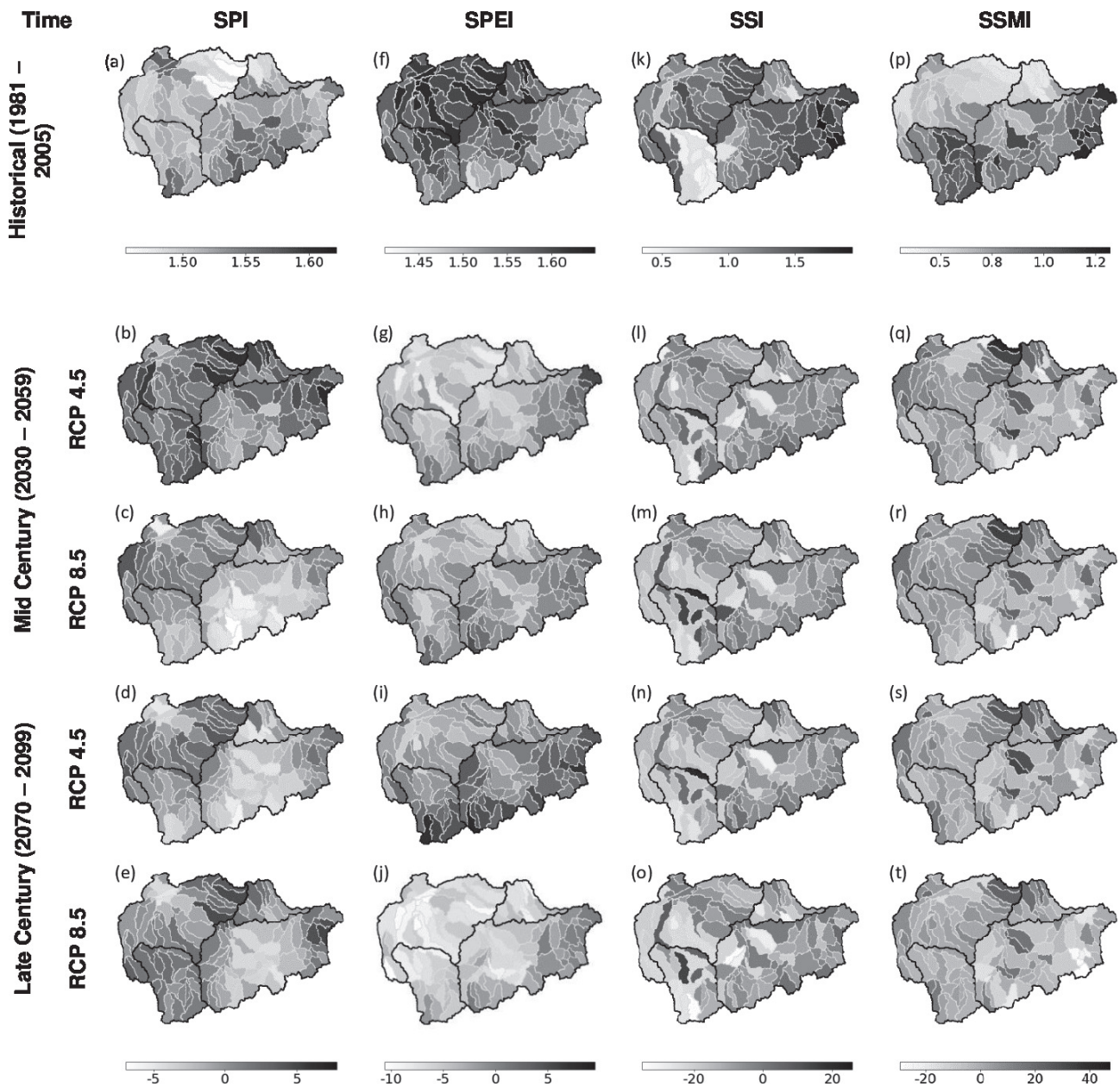


Fig. 3. Drought frequencies (number of drought events per year) for different climate scenarios and time periods in the URB; Mid Century and Late Century maps indicate the percentage change in projected drought frequency compared to the historical drought frequency.

have been reported (Dalton and Fleishman, 2021).

3.2. SWAT model results

The SWAT model of the URB was calibrated for streamflow, reservoir storage, and crop yield. The URB SWAT model performed well in simulating and predicting streamflow. Calibration of the SWAT model was done for the years 1999 to 2008, and the Nash-Sutcliffe efficiency for the calibration varied from 0.47 to 0.98. Validation of the model was done for the years 2009 to 2019, with Nash-Sutcliffe efficiency values ranging between 0.42 to 0.99. The percentage bias for the calibration and validation obtained is within 30 percent.

SWAT outputs, namely, streamflow, soil moisture, and potential evapotranspiration, were obtained for each sub-basin, and their average annual values were computed for the four zones (Table S4 in ESM). The trend analysis was performed on the model ensemble average values for the zones using the Mann-Kendall trend test at a 5% significance level ($p < 0.05$). Streamflow showed an increasing trend for zones 2 and 3 during the late-century for the RCP 4.5 scenario and no trend for the remaining scenarios. The ensemble average of the annual potential evapotranspiration showed an increasing trend in all four zones during all the scenarios except for RCP 4.5 late-century where it had no trend. The increasing trend in potential evapotranspiration is likely due to the

increasing temperatures in the basin. Both minimum and maximum temperatures have significant increasing trends throughout the basin during projected future conditions.

Similarly, the soil moisture exhibited a decreasing trend for Zones 1, 2, and 3 during two time periods: historical and RCP 8.5 late-century. It also showed decreasing trend for Zone 1 during RCP 4.5 and RCP 8.5 mid-century. Zone 4 had an increasing trend for soil moisture during the RCP 4.5 late century. The decreasing trend in soil moisture in most of the URB can be attributed to the increasing temperature and no significant trend in precipitation. As a result, there is more evaporative demand but no significant change in precipitation, vv the soil is under stress, which increases the need for irrigated agriculture in the region.

3.3. Drought characteristics for historical and projected climate scenarios

Historical and projected drought characteristics for the meteorological, hydrological, and agricultural drought in the URB were calculated for each sub-basin. The drought characteristics include drought frequency (average), drought duration (average and maximum), and drought severity (average and maximum). The computed results include the ensemble

average value of the drought characteristic from 10 models. Drought characteristics in the URB computed at the sub-basin level were aggregated to a zonal level consisting of four zones. Figure S3 in the ESM summarizes the projected short-term drought characteristics (frequency, duration, and severity) for the mid-century and late-century periods for RCP 4.5 and 8.5 scenarios in the URB. Short-term meteorological drought characteristics based on the SPI and SPEI display opposite behavior in most zones and projected scenarios. This behavior of the SPI and SPEI was also observed in a previous study from the Willamette River Basin in Oregon (Ahmadalipour et al., 2017a). The next section presents a summary of the results and insights obtained from our analysis.

3.3.1. Drought frequency

Figure 3 shows the drought frequencies for different climate scenarios and time periods in the URB. Historically observed average meteorological drought frequencies in the basin for the SPI and SPEI are 1.52 and 1.28 droughts per year, respectively. SPI-based drought frequency in the future scenarios is projected to increase by up to 3%, with a decrease during some scenarios for Zones 1, 2, and 4. SPEI-based meteorological drought frequency is projected in

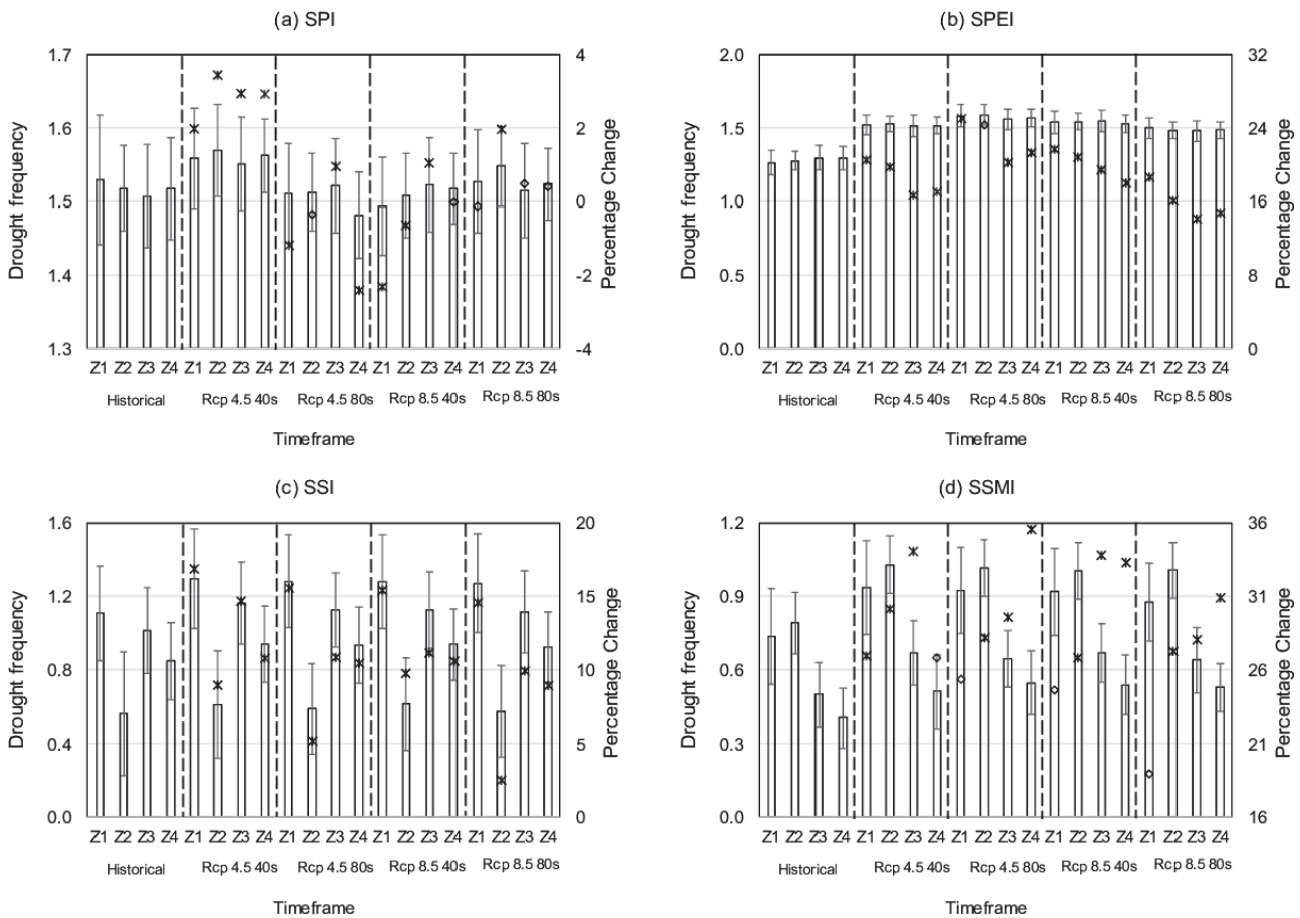


Fig. 4. Summary of average drought frequencies (number of drought events per year) expressed as bars plots (mean) with error bars (std.dev.) for different scenarios in the URB. The secondary y-axis represents the percentage change relative to the historical time period. The changes represented by an asterisk symbol were found to be statistically significant at the 5% significance level, whereas the changes represented by a diamond symbol were not statistically significant

future scenarios to increase by 14%–21% over the historical period, with the greatest increase in the southern sub-basins in Zones 1 and 2. These sub-basins have higher precipitation deficits caused by higher potential evapotranspiration and relatively unchanged precipitation during the late-century RCP 4.5 period compared to neighboring sub-basins, resulting in more SPEI-based droughts. Sub-basins in Zones 3 and 4 have more frequent SPEI-based meteorological drought whereas the sub-basins in the eastern and southeastern parts (with proximity to blue mountains) have somewhat less frequent meteorological droughts during the historical period.

Overall, the URB shows a higher drought frequency for meteorological drought (average: 1.5 yr⁻¹) in the historical

period than hydrological (average: 0.9 yr⁻¹) or agricultural drought (average: 0.60 yr⁻¹). Figure 4 shows changes in drought frequencies between the various scenarios for all the zones in the URB. Zone 2 has a much lower hydrological drought frequency (0.56 yr⁻¹) in the historical period than other zones. The projected hydrological drought frequency increased by an average of 11% in the projected scenarios, whereas the agricultural drought frequency increased by an average of 28% in the projected scenarios over the historical scenario.

3.3.2. Average drought duration

Figure 5 shows the average drought duration of short-

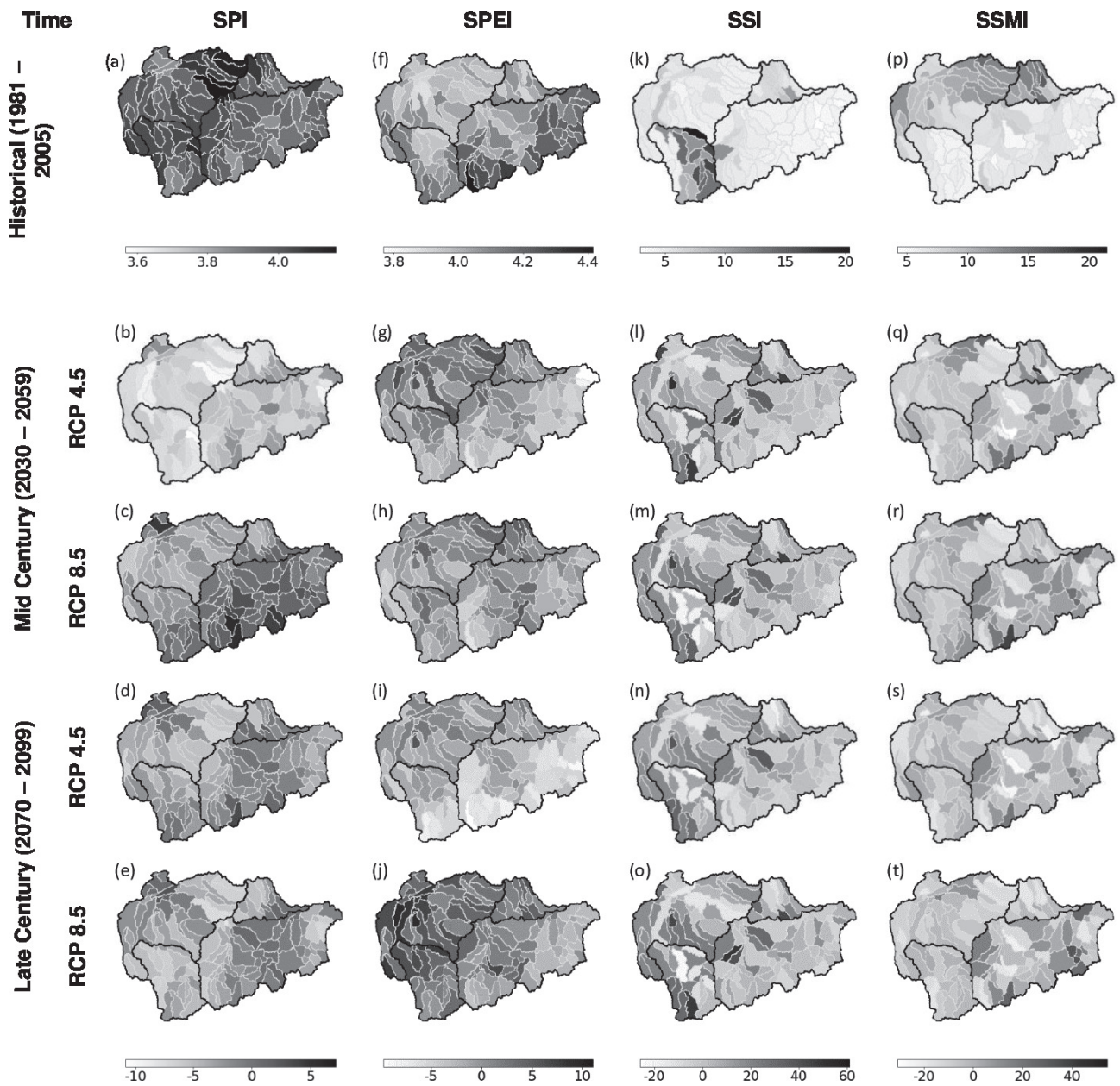


Fig. 5. Average drought durations (months per drought) for different climate scenarios and time periods in the URB; Mid Century and Late Century maps indicate the percentage change in projected average drought duration compared to the historical average drought duration.

term droughts for different scenarios and time periods in the URB. The average drought duration based on short-term (seasonal) anomalies for meteorological drought is shorter (average: 4 months) compared to hydrological (average: 7 months) and agricultural drought (average: 9 months) for the historical period. This means that anomalous seasonal (3-month) precipitation, evapotranspiration, soil moisture, etc., can have a lasting impact (from 4 to 9 months) on the drought conditions in the historical period. Short-term hydrological droughts during the historical period in the eastern sub-basins of Zone 2 have a longer duration of 12–20 months, which is much higher compared to sub-basins in other zones. Tributaries and streams of the Umatilla River in Zone 2 are characterized by low flow and are hydrologically isolated from other streams and zones. Thus, any anomaly in the streamflow lasts longer in this part of the URB than in Zones 3 and 4, which are more hydrologically connected.

Historically, the average short-term meteorological drought duration observed in the basin for the SPI and SPEI is 3.98 and 4.04 months per drought, respectively. The average duration for short-term SPI-based meteorological

droughts is projected to increase by up to 7% in future scenarios, with more sub-basins in the southern half of the basin (Zones 1 and 2) seeing an uptick in drought durations. Northern sub-basins in Zone 3 are projected to experience a decrease in their average drought duration by an average of 5% in RCP 4.5 scenarios compared to the historical period. The average duration of SPEI-based drought is projected to increase in most of the future scenarios by up to 6%, compared to the historical scenario, with the greatest increases seen in RCP 8.5 scenarios for Zones 3 and 4.

Figure 6 shows changes in average drought durations between the various scenarios for all the zones in the URB. The URB shows a higher average drought duration for hydrological drought in the historical period for Zone 2 (11.4 months per drought) compared to other zones. Average hydrological drought duration has increased in future scenarios compared to the historical period by an average of 8%. Projected average drought durations in future scenarios increase by more than 10%, on average, in Zones 3 and 4, whereas Zones 1 and 2 show lower increases. Average agricultural drought duration has decreased in future scenarios by an average of 4%. Zones 3 and 4 have much high average

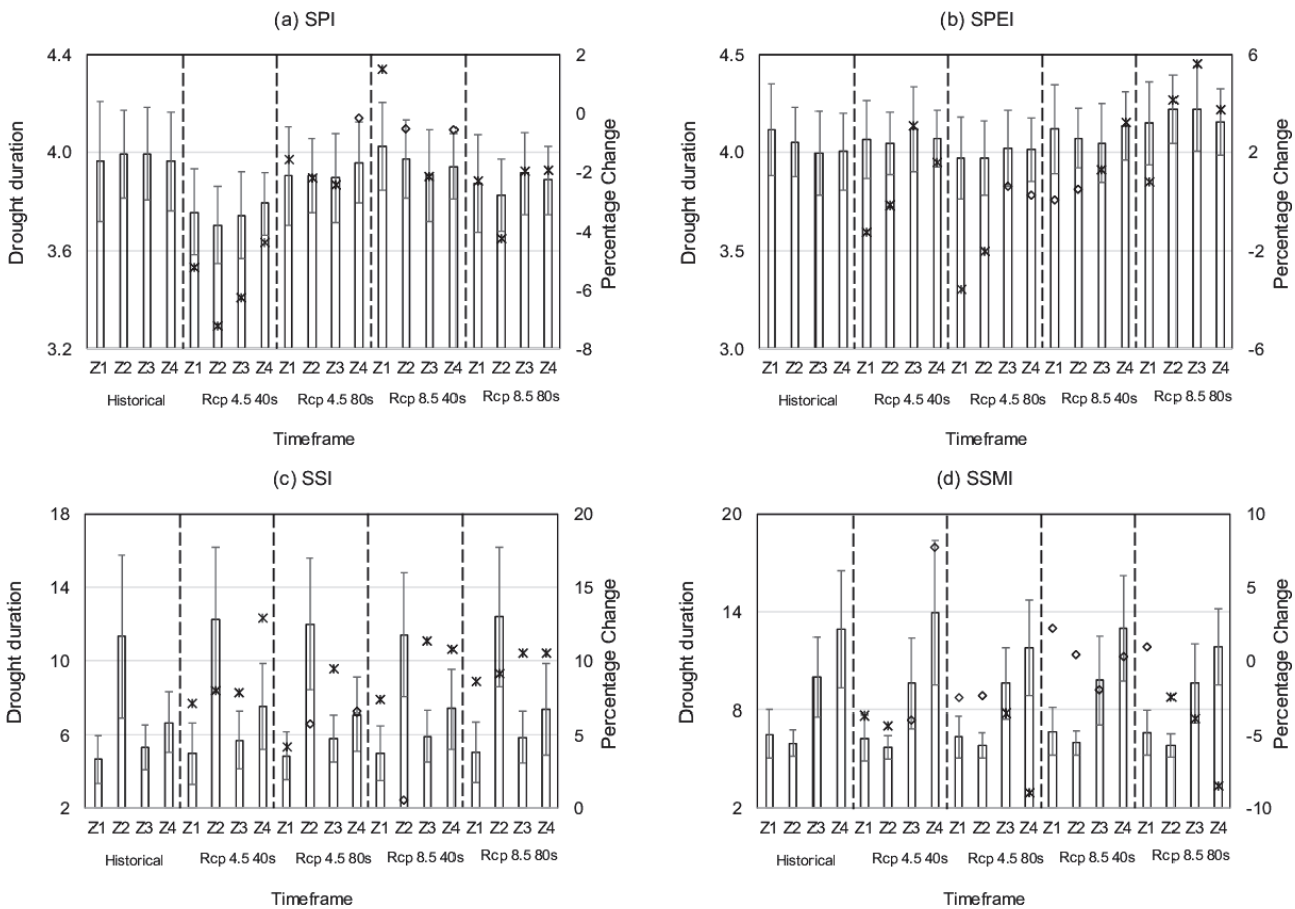


Fig. 6. Summary of average drought durations (months per drought) expressed as bars plots (mean) with error bars (std. dev.) for different scenarios in the URB. The secondary y-axis represents the percentage change relative to the historical time period. The changes represented by an asterisk symbol were found to be statistically significant at a 5% significance level, whereas the changes represented by a diamond symbol were not statistically significant.

agricultural drought durations (10 and 13 months per drought, respectively) in the historical period compared to other zones.

3.3.3. Average drought severity

Figure 7 presents the average drought severity in the URB for different scenarios. The average historical drought severity for meteorological drought (average severity of 3.2) is lower than the hydrological (average severity of 5.3) and agricultural drought (average severity of 7.6). The average meteorological drought severity based on the SPI is projected to decrease by up to 4% in future scenarios. In contrast, the drought severity based on the SPEI is projected to increase

in most sub-basins for future scenarios by up to 6%. It is evident that SPI-based short-term meteorological drought severity is projected to increase in the southern sub-basins in Zone 1 and northern sub-basins in Zone 3 (near the outlet of the Umatilla River) by up to 5% in future scenarios. SPEI-based average drought severity is projected to increase by up to 10% in most sub-basins throughout the URB during the late-century RCP 8.5 scenario.

Similarly, the average severity of projected hydrological droughts has increased by an average of 12%. In contrast, the average severity of the agricultural drought has decreased by up to 12% in future scenarios compared to the historical period, with Zone 4 having the most reduction in

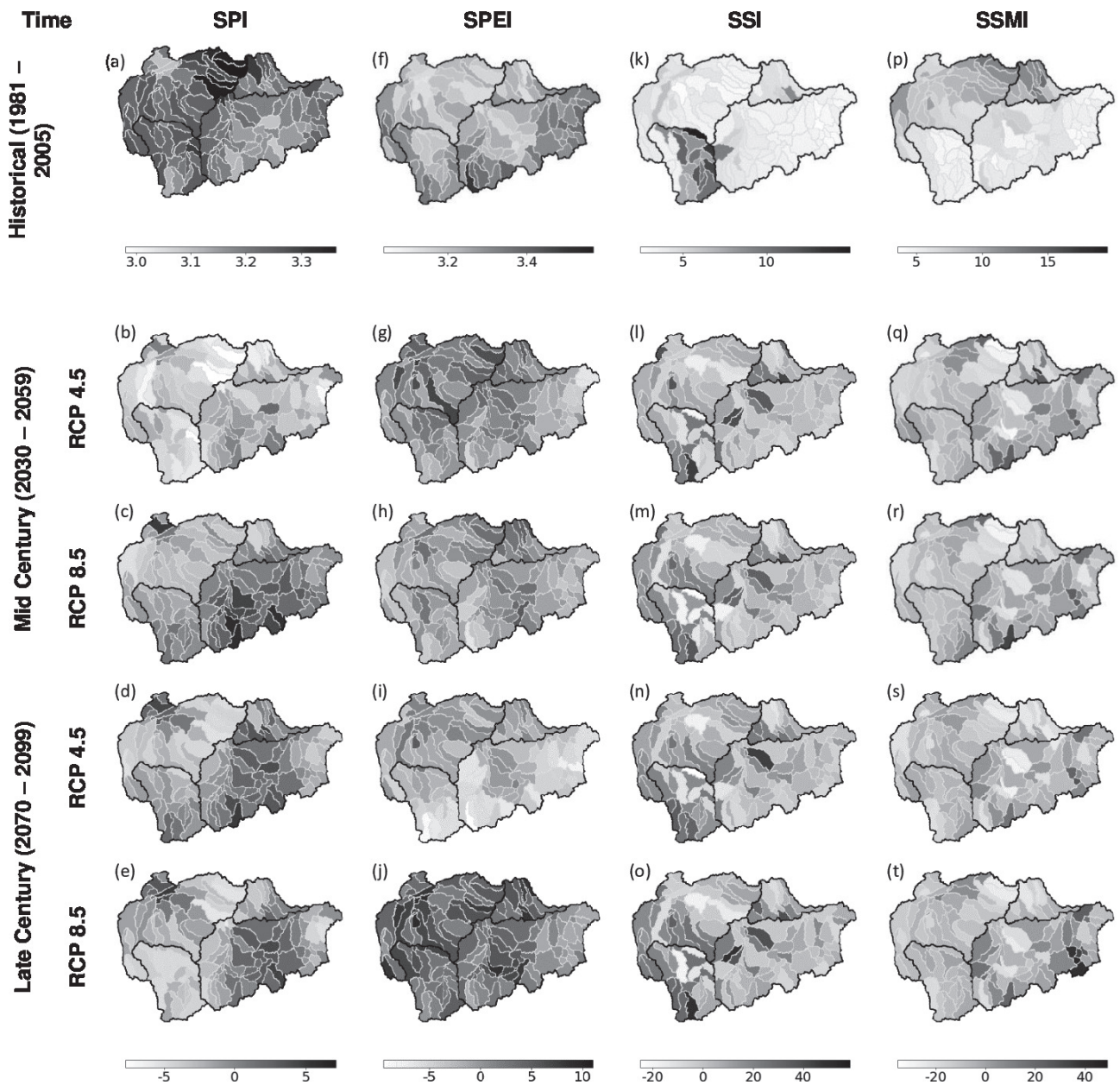


Fig. 7. Average drought severities (severity per drought) for different climate scenarios and time periods in the URB; Mid Century and Late Century maps represent the percentage change in projected average drought severity compared to the historical average drought severity.

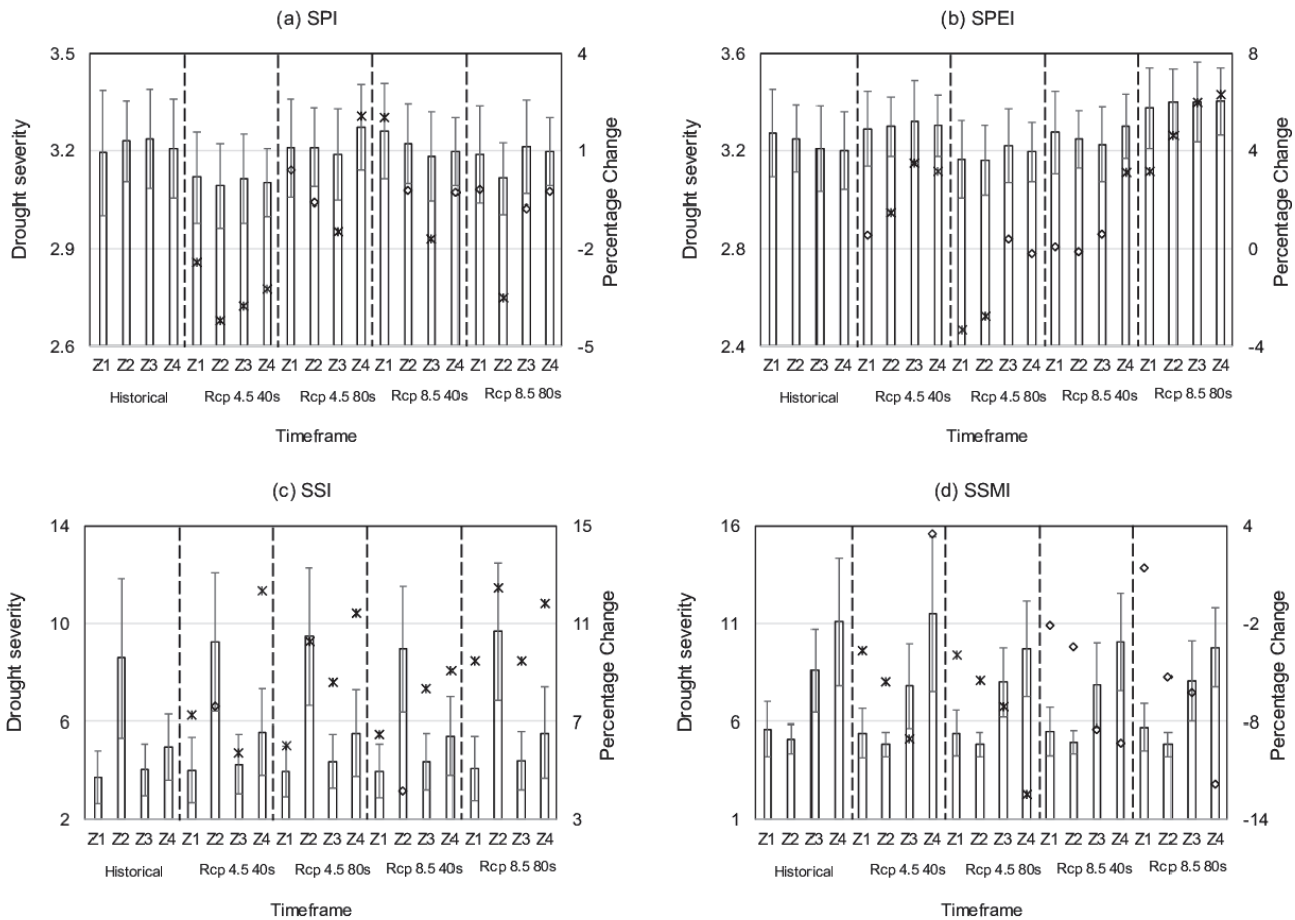


Fig. 8. Summary of average drought severities (severity per drought) expressed as bars plots (mean) with error bars (std. dev.) for different scenarios in the URB. The secondary y-axis represents the percentage change relative to the historical time period. The changes, represented by an asterisk symbol, were found to be statistically significant at a 5% significance level, whereas the changes represented by a diamond symbol were not statistically significant.

average severity. Figure 8 shows changes in average drought severity between various scenarios for all zones in the URB.

3.3.4. *Maximum drought duration and maximum drought severity*

The maximum drought duration in the URB exhibited similar behavior to average drought duration (Fig. S4 in the ESM), and the maximum drought severity also showed similar behavior to the average drought severity in the basin for historical and future scenarios (Fig. S5 in the ESM).

3.4. *Drought propagation*

Figure 9 shows the propagation time from meteorological drought to hydrological and agricultural droughts in the URB. For most sub-basins in Zones 1 and 3, the maximum correlation between the SPI and SSI occurs at the SPI scale of 4–6 months, indicating a drought propagation time of 4–6 months between the precipitation and streamflow drought. There is a higher propagation time in Zones 2 and 4. The propagation time for the future scenarios increased by 1 month in Zone 2 and decreased by 1 month in Zone 1. Similarly, the drought propagation from SPI to SSMI occurs

at the SPI scale of 6–8 months for most of the sub-basins in Zones 1 and 2.

Drought propagation in a basin can be affected by the prior condition of climate, basin characteristics, and human influences (Zhang et al., 2022). Climatic factors may include weather patterns and seasonality, whereas catchment characteristics may include the elevation, slope, land use/land cover, type of aquifer, and hydraulic conductivity of the soil. Human influences affecting drought propagation may include water diversion, groundwater abstraction, and irrigation practices. The strong linkage between meteorological drought and hydrological drought can be seen in Zones 3 and 4, as evidenced by smaller propagation times for the hydrological drought. This can be explained by the increased evapotranspiration and low precipitation in regions dominated by agricultural practices. The smaller response time in Zone 1 from meteorological drought to hydrological drought can be attributed to the higher slope (up to 56.5%) compared to other parts of the basin (Fig. 1c).

Table S6 in the ESM summarizes the average drought propagation time for all the time periods and RCP scenarios for different zones in the URB. The propagation time of mete-

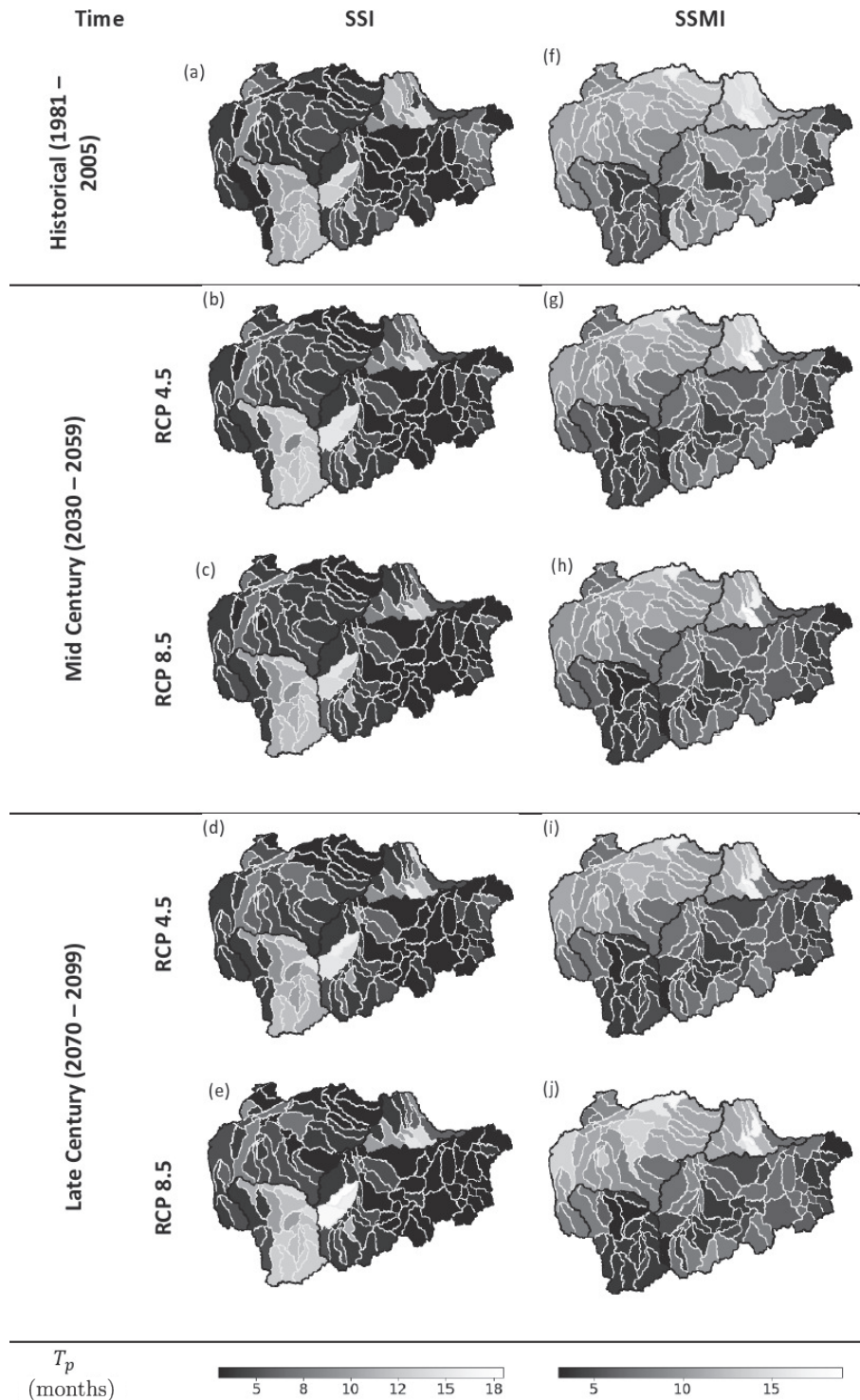


Fig. 9. Drought propagation time from meteorological (SPI) to hydrological (SSI) and agricultural (SSMI) droughts.

orological drought to hydrological drought ranges from 4 to 9 months during the historical period and increases up to 10 months in the projected future scenarios. Similarly, the propagation time for meteorological drought to agricultural drought decreases from 5–14 months in the historical period to 4–13 months in the projected scenarios.

The lag time between meteorological drought and hydro-

logical drought for future scenarios in Zone 2 increases to 10 months from 9 months during the historical period. Other zones show no change or decrease in lag time (lead) for future scenarios. This behavior in Zone 2 reflects how physical factors such as soil and initial moisture conditions may affect runoff generation, aside from precipitation. Zone 2 is dominated by soils of hydrologic groups C (clay loam

and shallow sandy loam) and D (heavy plastic clays), which have slow infiltration rates and runoff is more sensitive to precipitation (Fig. 1d). The increase in the lag time in Zone 2 reflects that hydrological drought is strongly connected with meteorological drought.

The lag time between meteorological drought and agricultural drought for future scenarios in all the zones has decreased compared to the historical period in a few cases. The decrease in this drought propagation time can be attributed to the effect of high temperatures in future scenarios. Higher temperatures can lead to increased surface evapotranspiration and could decrease surface soil moisture, thus making drought propagation faster in the projected future scenarios (Ho et al., 2021). This decrease in drought propagation time between meteorological and agricultural drought means that a smaller decrease in the precipitation might be enough to result in the loss of a larger amount of soil moisture and affect agricultural productivity. As a result, a larger area of agricultural lands in the basin will likely become even more irrigation dependent for agricultural production in future scenarios putting stress on the basin's water supply and physical infrastructure.

4. Conclusion

This study aimed to characterize the three types of physical droughts: meteorological drought, agricultural drought, and hydrological drought in the Umatilla River Basin in northeastern Oregon and to investigate the drought propagation for the historical and future projected scenarios. Drought characteristics in the future were determined using downscaled CMIP5 climate datasets from 10 GCMs. The SWAT model of the basin was calibrated for streamflow, reservoir storage, and crop yield using PRISM climate data, and both historical and future scenarios were simulated by forcing the respective future climate data to the SWAT model. Drought characteristics (frequency, duration, and severity) were analyzed using multiple drought indices: SPI, SPEI, SSI, and SSMI. The propagation of meteorological drought to agricultural and hydrological droughts in the basin was also studied by performing a correlation analysis between drought indicators to identify the drought propagation times.

Our results indicate that changes in short-term drought frequency, duration, and severity are expected in the future in the basin. Short-term meteorological droughts are projected to become more prevalent in the basin, but the SPI and SPEI indicate differing results. Short-term hydrological drought is projected to become more frequent and more severe throughout the basin. Short-term agricultural drought is projected to be more frequent but less severe in future projected conditions. For short-term droughts, the propagation time from meteorological to hydrological drought is found to be less than the propagation time from meteorological to agricultural drought in most sub-basins.

The analysis conducted in this study is a step towards understanding the drought characteristics in the URB at present and in the future. In addition to the changing climate,

factors such as basin slope and hydraulic conductivity that could change due to land use and land cover changes might influence the drought propagation time in the basin in the future, which needs to be incorporated in upcoming studies. Long-term drought-related studies are also required for this region so that we can fully understand the effects of drought on various water-dependent sectors in the region. Future studies should specifically explore how the changing nature of drought characteristics might stress the food-energy-water systems in the basin by increasing the need for agricultural irrigation.

Acknowledgements. We gratefully acknowledge the financial support received from the U.S. Department of Agriculture (USDA) National Institute of Food and Agriculture (NIFA), USA (Grant No.2017-67003-26057) via an interagency partnership between USDA-NIFA and the National Science Foundation (NSF) on the research program Innovations at the Nexus of Food, Energy and Water Systems. Part of this work was also funded by the Ministry of Education, Government of India through the Scheme for Promotion of Academic and Research Collaboration (SPARC) project grant (SPARC/2018-2019/P1080/SL).

Electronic supplementary material: Supplementary material is available in the online version of this article at <https://doi.org/10.1007/s00376-023-2302-8>.

REFERENCES

- Abatzoglou, J. T., and D. E. Rupp, 2017: Evaluating climate model simulations of drought for the northwestern United States. *International Journal of Climatology*, **37**, 910–920, <https://doi.org/10.1002/joc.5046>.
- Ahmadalipour, A., A. Rana, H. Moradkhani, and A. Sharma, 2017b: Multi-criteria evaluation of CMIP5 GCMs for climate change impact analysis. *Theor. Appl. Climatol.*, **128**(1–2), 71–87, <https://doi.org/10.1007/s00704-015-1695-4>.
- Ahmadalipour, A., H. Moradkhani, and M. C. Demirel, 2017a: A comparative assessment of projected meteorological and hydrological droughts: Elucidating the role of temperature. *J. Hydrol.*, **553**, 785–797, <https://doi.org/10.1016/j.jhydrol.2017.08.047>.
- Apurv, T., M. Sivapalan, and X. Cai, 2017: Understanding the role of climate characteristics in drought propagation. *Water Resour. Res.*, **53**(11), 9304–9329, <https://doi.org/10.1002/2017WR021445>.
- Arnold, J. G., and Coauthors, 2012: SWAT: Model use, calibration, and validation. *Transactions of the ASABE*, **55**(4), 1491–1508, <https://doi.org/10.13031/2013.42256>.
- Arnold, J. G., J. R. Kiniry, R. Srinivasan, J. R. Williams, E. B. Haney, and S. L. Neitsch, 2013: Soil & water assessment tool: Input/output documentation. version 2012. TR-439.
- Ault, T. R., 2020: On the essentials of drought in a changing climate. *Science*, **368**(6488), 256–260, <https://doi.org/10.1126/science.aaz5492>.
- Clifton, C. F., K. T. Day, C. H. Luce, G. E. Grant, M. Safeeq, J. E. Halofsky, and B. P. Staab, 2018: Effects of climate change on hydrology and water resources in the Blue Mountains, Oregon, USA. *Climate Services*, **10**, 9–19, <https://doi.org/10.1016/j.cliser.2018.03.001>.

- Dalton, M., 2020: Future climate projections: Umatilla County. Oregon Climate Change Research Institute. Oregon State University, Corvallis, Oregon. Available online at https://ir.library.oregonstate.edu/concern/technical_reports/tq57p0384.
- Dalton, M. M., and E. Fleishman, 2021: Fifth Oregon climate assessment. Oregon Climate Change Research Institute. Oregon State University, Corvallis, Oregon. <https://doi.org/10.5399/osu/1160>.
- Ding, Y., M. J. Hayes, and M. Widhalm, 2011: Measuring economic impacts of drought: A review and discussion. *Disaster Prevention and Management*, **20**(4), 434–446, <https://doi.org/10.1108/09653561111161752>.
- Drought.gov, 2021: Monitoring Drought. <https://www.drought.gov/what-is-drought/monitoring-drought>.
- European Commission, 2020: EDO indicator factsheet: Standardized precipitation index. Available online at https://edo.jrc.ec.europa.eu/documents/factsheets/factsheet_spi.pdf.
- Hayes, M. J., M. D. Svoboda, D. A. Wihite, and O. V. Van-yarkho, 1999: Monitoring the 1996 drought using the Standardized Precipitation Index. *Bull. Amer. Meteor. Soc.*, **80**(3), 429–438, [https://doi.org/10.1175/1520-0477\(1999\)080<0429:MTDUTS>2.0.CO;2](https://doi.org/10.1175/1520-0477(1999)080<0429:MTDUTS>2.0.CO;2).
- Ho, S., L. Tian, M. Disse, & Y. Tuo, 2021: A new approach to quantify propagation time from meteorological to hydrological drought. *J. Hydrol.*, **603**, 127056, <https://doi.org/10.1016/j.jhydrol.2021.127056>.
- Hussain, M., and I. Mahmud, 2019: pyMannKendall: a python package for non parametric Mann Kendall family of trend tests. *Journal of Open Source Software*, **4**(39), 1556, <https://doi.org/10.21105/joss.01556>.
- Indiana Department of Natural Resources, 2022: Explanation of Standard Precipitation Index (SPI). Available online at <https://www.in.gov/dnr/water/water-availability-use-rights/water-resource-updates/monthly-water-resource-summary/explanation-of-standard-precipitation-index-spi>.
- Jehanzaib, M., M. N. Sattar, J. H. Lee, and T. W. Kim, 2020: Investigating effect of climate change on drought propagation from meteorological to hydrological drought using multi-model ensemble projections. *Stochastic Environmental Research and Risk Assessment*, **34**(1), 7–21, <https://doi.org/10.1007/s00477-019-01760-5>.
- Keyantash, J., and J. A. Dracup, 2002: The quantification of drought: An evaluation of drought indices. *Bull. Amer. Meteor. Soc.*, **83**(8), 1167–1180, <https://doi.org/10.1175/1520-0477-83.8.1167>.
- Kwak, J., S. Kim, J. Jung, V. P. Singh, D. R. Lee, and H. S. Kim, 2016: Assessment of meteorological drought in Korea under climate change. *Advances in Meteorology*, **2016**, 1879024, <https://doi.org/10.1155/2016/1879024>.
- Leeper, R. D., and Coauthors, 2022: Characterizing U.S. drought over the past 20 years using the U.S. drought monitor. *International Journal of Climatology*, **42**, 6616–6630, <https://doi.org/10.1002/joc.7653>.
- Li, P., N. Omani, I. Chaubey, and X. M. Wei, 2017: Evaluation of drought implications on ecosystem services: Freshwater provisioning and food provisioning in the upper Mississippi river basin. *International Journal of Environmental Research and Public Health*, **14**(5), 496, <https://doi.org/10.3390/ijerph14050496>.
- McKee, T. B., J. Nolan, and J. Kleist, 1993: The relationship of drought frequency and duration to time scales. Proceedings of the Eighth Conf. on Applied Climatology, **7**(22), 179–183.
- Mishra, A. K., and V. P. Singh, 2010: A review of drought concepts. *J. Hydrol.*, **391**(1–2), 202–216, <https://doi.org/10.1016/j.jhydrol.2010.07.012>.
- Modarres, R., 2007: Streamflow drought time series forecasting. *Stochastic Environmental Research and Risk Assessment*, **21**(3), 223–233, <https://doi.org/10.1007/s00477-006-0058-1>.
- Mukherjee, S., A. Mishra, and K. E. Trenberth, 2018: Climate change and drought: A perspective on drought indices. *Current Climate Change Reports*, **4**(2), 145–163, <https://doi.org/10.1007/s40641-018-0098-x>.
- National Drought Mitigation Center, 2021: Types of drought. <https://drought.unl.edu/Education/DroughtIn-depth/TypesofDrought.aspx>.
- National Drought Mitigation Center, 2022: Measuring drought. <https://drought.unl.edu/ranchplan/DroughtBasics/WeatherandDrought/MeasuringDrought.aspx>.
- Neitsch, S. L., J. G. Arnold, J. R. Kiniry, and J. R. Williams, 2011: Soil and water assessment tool: Theoretical documentation, version 2009. TR-406.
- NOAA National Centers for Environmental Information, 2022: U. S. billion-dollar weather and climate disasters. <https://doi.org/10.25921/stkw-7w73>.
- Oregon.gov, 2021: Drought. <https://www.oregon.gov/owrd/programs/climate/droughtwatch/pages/default.aspx>.
- Oregon.gov, 2022: Groundwater administrative areas/critical groundwater areas. <https://www.oregon.gov/owrd/programs/gww/gw/pages/adminareasandcriticalgwareas.aspx>.
- Oregon Water Resources Department, 2022: Public declaration status report. Drought Declarations. Available online at https://apps.wrd.state.or.us/apps/wr/wr_drought/declaration_status_report.aspx.
- Palmer, W. C., 1965: Meteorological drought. Office of Climatology Research Paper No. 45.
- State of Oregon, 2016: Report of the task force on drought emergency response. House Bill 4113 (2006).
- Sun, P., Q. Zhang, V. P. Singh, M. Z. Xiao, and X. Y. Zhang, 2017: Transitional variations and risk of hydro-meteorological droughts in the Tarim River basin, China. *Stochastic Environmental Research and Risk Assessment*, **31**(6), 1515–1526, <https://doi.org/10.1007/s00477-016-1254-2>.
- Sun, P., Z. C. Ma, Q. Zhang, V. P. Singh, and C. Y. Xu, 2022: Modified drought severity index: Model improvement and its application in drought monitoring in China. *J. Hydrol.*, **612**, 128097, <https://doi.org/10.1016/j.jhydrol.2022.128097>.
- Svoboda, M., and Coauthors, 2002: The drought monitor. *Bull. Amer. Meteor. Soc.*, **83**(8), 1181–1190, <https://doi.org/10.1175/1520-0477-83.8.1181>.
- Tilt, J. H., H. A. Mondo, N. A. Giles, S. Rivera, and M. Babbar-Sebens, 2022: Demystifying the fears and myths: The co-production of a regional food, energy, water (FEW) nexus conceptual model. *Environmental Science & Policy*, **132**, 69–82, <https://doi.org/10.1016/j.envsci.2022.02.011>.
- USDA, 2005: Umatilla – 17070103, 8-digit hydrologic unit profile. Available online at https://www.nrcs.usda.gov/wps/PA_NRCSCConsumption/download/?cid=nrcseprd1482439&ext=pdf.
- van Loon, A. F., 2013: On the Propagation of Drought: How Climate and Catchment Characteristics Influence Hydrological Drought Development and Recovery. PhD dissertation, Wageningen University.
- van Loon, A. F., 2015: Hydrological drought explained. *WIREs*

- Water*, **2**(4), 359–392, <https://doi.org/10.1002/wat2.1085>.
- van Loon, A. F., S. W. Ploum, J. Parajka, A. K. Fleig, E. Garnier, G. Laaha, and H. A. J. van Lanen, 2015: Hydrological drought types in cold climates: Quantitative analysis of causing factors and qualitative survey of impacts. *Hydrology and Earth System Sciences*, **19**(4), 1993–2016, <https://doi.org/10.5194/hess-19-1993-2015>.
- Vicente-Serrano, S. M., S. Beguería, and J. I. López-Moreno, 2010: A multiscalar drought index sensitive to global warming: The standardized precipitation evapotranspiration index. *J. Climate*, **23**(7), 1696–1718, <https://doi.org/10.1175/2009JCLI2909.1>.
- Williams, A. P., B. I. Cook, and J. E. Smerdon, 2022: Rapid intensification of the emerging southwestern North American megadrought in 2020–2021. *Nature Climate Change*, **12**, 232–234, <https://doi.org/10.1038/s41558-022-01290-z>.
- WMO, and GWD, 2016: Handbook of drought indicators and indices. *Integrated Drought Management Tools and Guidelines Series 2*, M. Svoboda and B. A. Fuchs, Eds., Integrated Drought Management Programme (IDMP). Available online at https://library.wmo.int/doc_num.php?explnum_id=3057.
- Wood, A. W., L. R. Leung, V. Sridhar, and D. P. Lettenmaier, 2004: Hydrologic implications of dynamical and statistical approaches to downscaling climate model outputs. *Climatic Change*, **62**(1–3), 189–216, <https://doi.org/10.1023/B:CLIM.0000013685.99609.9e>.
- Xu, Y. P., L. Wang, K. W. Ross, C. L. Liu, and K. Berry, 2018: Standardized Soil Moisture Index for drought monitoring based on soil moisture active passive observations and 36 Years of North American Land Data Assimilation System data: A case study in the Southeast United States. *Remote Sensing*, **10**(3), 301, <https://doi.org/10.3390/rs10020301>.
- Xu, Y., X. Zhang, X. Wang, Z. C. Hao, V. P. Singh, and F. H. Hao, 2019: Propagation from meteorological drought to hydrological drought under the impact of human activities: A case study in northern China. *J. Hydrol.*, **579**, 124147, <https://doi.org/10.1016/j.jhydrol.2019.124147>.
- Yevjevich, V., 1967: An objective approach to definitions and investigations of continental hydrologic droughts. No. 23. Doctoral Dissertation. Colorado State University, Fort Collins, Colorado. Available online at https://www.engr.colostate.edu/ce/facultystaff/yevjevich/papers/HydrologyPapers_n23_1967.pdf.
- Zhang, X., Z. C. Hao, V. P. Singh, Y. Zhang, S. F. Feng, Y. Xu, and F. H. Hao, 2022: Drought propagation under global warming: Characteristics, approaches, processes, and controlling factors. *Science of the Total Environment*, **838**, 156021, <https://doi.org/10.1016/j.scitotenv.2022.156021>.
- Zhao, T. B., and A. G. Dai, 2015: The magnitude and causes of global drought changes in the twenty-first century under a low-moderate emissions scenario. *J. Climate*, **28**(11), 4490–4512, <https://doi.org/10.1175/JCLI-D-14-00363.1>.